Exploration of BioMat-X

Open Exploration

Open Access Original Article

Decellularized bone extracellular matrix as a promising natural substrate for bone tissue engineering

Aylin Kara Özenler[1,2,3*], Hasan Havitcioglu[3], Funda Tihminlioglu[4*]

[1]Department of Bioengineering, Izmir Institute of Technology, 35430 Izmir, Turkey
[2]Department of Orthopedics, University Medical Center Utrecht, 3584 CX Utrecht, the Netherlands
[3]Department of Orthopedics and Traumatology, Dokuz Eylul University, 35340 Izmir, Turkey
[4]Department of Chemical Engineering, Izmir Institute of Technology, 35340 Izmir, Turkey

***Correspondence:** Aylin Kara Özenler, Department of Orthopedics, University Medical Center Utrecht, 3584 CX Utrecht, the Netherlands. a.karaozenler@umcutrecht.nl; Funda Tihminlioglu, Department of Chemical Engineering, Izmir Institute of Technology, Urla, 35340 Izmir, Turkey. fundatihminlioglu@iyte.edu.tr
Academic Editor: Omid Akhavan, Sharif University of Technology, Iran
Received: March 31, 2025 **Accepted:** August 11, 2025 **Published:** September 11, 2025

Cite this article: Kara Özenler A, Havitcioglu H, Tihminlioglu F. Decellularized bone extracellular matrix as a promising natural substrate for bone tissue engineering. Explor BioMat-X. 2025;2:101345. https://doi.org/10.37349/ebmx.2025.101345

Abstract

Aim: The decellularization process aims to remove cellular components from the tissues while preserving the ultrastructural composition of the extracellular matrix (ECM). Decellularization of bone is gaining attention as a biological scaffold due to its unique histoarchitecture, which consists of both organic and inorganic compounds. This study aims to develop a biological bone ECM using a novel decellularization method for bone regeneration.

Methods: Rabbit and rat bone tissues were decellularized using a novel process that combines physical, chemical, and enzymatic methods with 0.1% SDS. Bone tissues were evaluated in terms of histology, biochemistry, and biomechanical tests, both before and after decellularization. Additionally, decellularized bone substitutes were recellularized with preosteoblast cells to assess the cytotoxic effect of the decellularization process.

Results: Our method effectively removes cellular components while preserving both organic and inorganic compounds. We achieved a 95% in DNA content for rabbit bone and 92% for rat bone. The biochemical and biomechanical properties remained unchanged, and mineralization features were preserved after decellularization. The cell culture results revealed that decellularized bone extracellular matrix (dbECM) is biocompatible, bioactive, and provides a suitable environment for cell growth.

Conclusions: This study demonstrates that our novel decellularization method effectively develops biological bone ECM containing both organic and inorganic compounds while utilizing minimal chemical concentration and incubation time. It is foreseen that the resulting decellularized bone could serve as a biological substitute, providing a favorable microenvironment for bone regeneration.

Keywords

decellularization, bone tissue, bone extracellular matrix, bone tissue engineering, mineralization

Introduction

Bone tissue engineering aims to repair defective bone tissues with scaffolds that can mimic the host tissue. Three-dimensional scaffolds should provide a similar morphological structure and porosity, suitable mechanical strength, biodegradable and bioactive, capable of mimicking bone tissue. The scaffold is expected to be non-toxic and biocompatible to ensure safe integration when implanted in the defective tissue [1]. Also, scaffold replaced the defect site is expected to be osteoconductive and osteoinductive [2–5]. In recent years, several synthetic and natural polymers and methods have been evaluated for the development of biomaterials for bone tissue engineering and regenerative medicine approaches. Synthetic polymers [poly(lactic acid), polycaprolactone, poly(glycolic acid), polyurethanes)] show restricted bioactive moieties to improve biocompatibility and regenerative capacity [6, 7]. To overcome this deficiency, functionalization methods have been used and mixed with the natural polymers or bioactive agents to produce composite biomaterials with physically and biologically better than single material-based ones [8–12]. As far as the bone is concerned, mineralization is a major important factor as well as biocompatibility and biodegradability for bone regeneration [13]. Therefore, biomaterials including hydroxyapatite (HAp), tricalcium phosphate, or derivatives are preferred due to improving the mineralization and mechanical properties to mimic the bone tissue. Moreover emerging approaches in tissue engineering, such as the use of extracellular matrices through decellularization, hold great potential for overcoming these challenges. [14–16].

Biological scaffolds developed by the decellularization method are widely studied due to the lack of immunological reactions, their mechanical strength is similar to native tissue, and the microstructure of the tissues is maintained [17]. The main purpose of the decellularization method is to remove the cellular components from the tissue without damaging the extracellular matrix (ECM) and biomechanical stress, as well as decreasing the antigenicity of the tissues. The natural ECM structure obtained by the decellularization method is a promising candidate as a more ideal carrier in terms of containing collagen, glycosaminoglycan (GAG), matrix proteins, and growth factors [16, 18]. Decellularization methods and their successful results were reported for the small intestine [14], the urinary bladder [19], the liver [20], the dermis [21], and esophagus transplants [22]. Tissues treated with different solutions to remove vital immunogenic cells can provide an optimum decellularized biological scaffold material for tissue engineering [23, 24]. The success of the decellularization process is largely related to tissue structures, methods used, chemicals, and their concentrations.

Different methods have been used for decellularization, including physical treatments (repetitive freeze-thaw, high pressure), chemical treatments (ionic, non-ionic solutions, hypotonic, hypertonic buffers), and enzymatic treatments (trypsin, collagenase, protease) [23, 25]. Repetitive freezing/thawing and high-pressure treatments can leave cell debris, and as a result, potential immunogenic reactions may occur. The combination of Triton-X with sodium dodecyl sulfate (SDS) has been reported to be highly effective in removing cellular components from tissues, however, this treatment may also lead to the loss or degradation of extracellular matrix components such as collagen and glycosaminoglycans (GAGs) [26]. SDS and other detergents or solvents like Triton-X or *tri-n*-butyl phosphate (TnBP) remove all cells and cellular debris [27, 28]. These frequently used chemicals are biocompatible and have been shown to support different levels of cellular growth [29]. When Triton-X, TnBP, and SDS are compared, it is seen that SDS is more effective in removing cell and cellular residues [29, 30]. In addition, it is seen that among the methods used, the best results are obtained by the chemical decellularization method; however, biomechanical properties were observed to be affected due to the deterioration in the ECM structure of the tissue [31]. Changes in biomechanical properties can adversely influence cellular activity and compromise the regeneration capacity of the tissue. The development of a decellularized bone scaffold has been motivated

by the need to improve the biocompatibility of allograft bone and the benefit of preserving the natural structure of bone.

Recently, several studies have been reported on bone tissue decellularization. These studies indicate that demineralization and decellularization processes are often applied in combination. The inorganic components that provide mineralization of tissue are damaged while separating the cellular components [32]. On the other hand, high amounts of detergent (0.5%, 1%, 2.5%) and mixing of different detergents were used for decellularization of the bone tissue [32–36]. These processes can cause damage in both organic and inorganic structures of bone. Bracey et al. [5] used chemical decellularization and oxidation methods to obtain osteoinductive bone scaffolds as well as to investigate the osteoinductive potential of decellularized bones in comparison to the demineralized scaffolds. It was reported that decellularized bone extracellular matrix (dbECM) had greater ALP enzyme activity and BMP2 expression, which indicated that decellularized scaffolds possessed osteoinductive potential compared to demineralized scaffolds [5]. High amounts of detergents cause breakdown of the ECM proteins and disrupted tissue morphology. Mattioli-Belmonte et al. [37] used both decellularization and demineralization methods with various chemicals such as sodium hypochlorite (for decellularization), hydrochloric acid, ammonia, and ammonium oxalate (for demineralization and decalcification). It was reported that ALP, Sox-2, osteocalcin, and Octamer-binding transcription factor, which are involved in the mineralization process, were decreased [37]. Besides, demineralization causes the removal of inorganic compounds, which are important for osteoinductivity [3, 5, 38, 39]. After demineralization, insufficient cellular functions can occur during bone regeneration [40]. Mineralization is the distinctive feature of bone tissue; however, this feature has not been considered in many decellularization studies.

The aim of the study is therefore to develop an effective decellularization method that preserves the natural organic and inorganic histoarchitecture of the bone tissue. Our novel decellularization method consists of physical, chemical, and enzymatic steps and enables decellularization of the bone with a minimum detergent concentration with a minimum incubation time. After the decellularization process, dbECM was recellularized to obtain a biological substrate that allows cell adhesion and proliferation. The schematic representation of the presented study is illustrated in Figure 1. For this purpose, rabbit and rat bone tissues were decellularized with 0.1% (w/v) SDS for 12 days and investigated histologically, biochemically, and biomechanically after decellularization. Moreover, cytocompatibility and osteoinductivity of the dbECM were evaluated by using MC3T3-E1 cells.

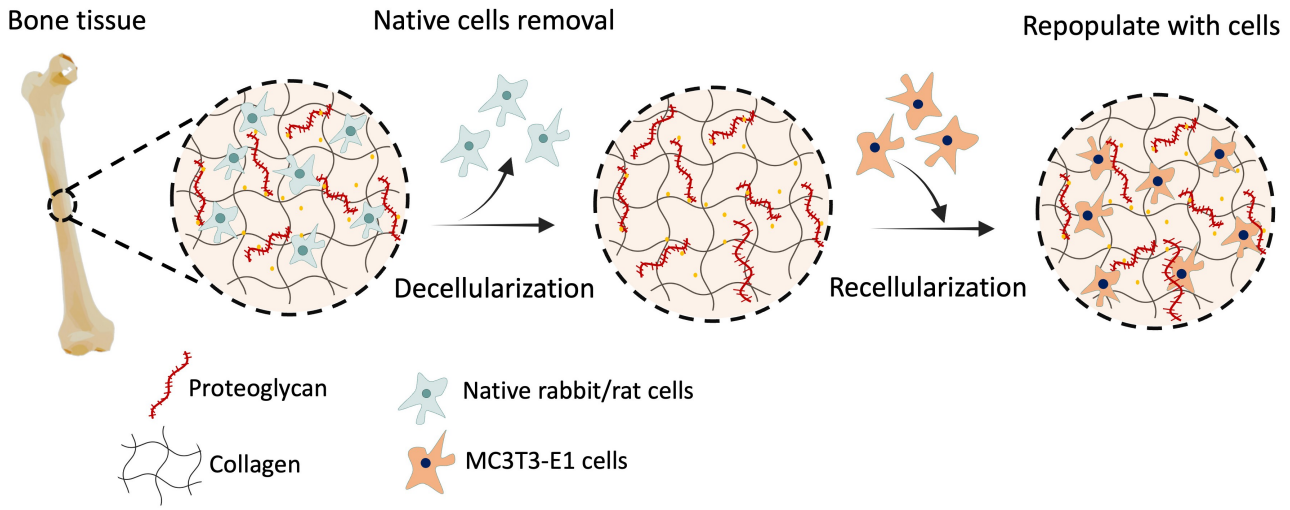

Figure 1. Schematic representation of decellularization and recellularization of the bone ECM.

Materials and methods

Collection of the bone samples

Rabbit and rat femur bones were used for decellularization. New Zealand White Rabbits (weight, 2.5–3.0 kg; female) and rats (weight, 150–200 g; female) were obtained from Dokuz Eylul University, Department of Laboratory Animal Science (Izmir, Turkey). All animal experiments were performed in accordance with the protocol accepted by the Experimental Animals Ethical Council of Dokuz Eylul University. The rabbits and rats were euthanized using an overdose of pentobarbital (200 mg/kg, IP for rats and 150 mg/kg, IV for rabbits), in accordance with AVMA Guidelines for the Euthanasia of Animals [41]. Rat and rabbit bone tissues were cut into 1 cm^3 pieces using an autopsy saw, and one of the adjacent pieces was used as a control, and the other as a sample. Bone tissues were stored in –20°C until further use.

Decellularization of the bone tissues

Decellularization was performed with a novel technique involving the combination of physical, chemical, and enzymatic methods with a minimum detergent concentration for 12 days. The novel technique firstly starts with a physical treatment method that was subjected to three freeze-thaw cycles, freezing at –80°C for 3 h and thawing at room temperature for 2 h. Then samples were incubated in a hypotonic buffer at 37°C for 24 h, followed by 0.1% (*w*/*v*) SDS in the presence of 0.1% (*w*/*v*) EDTA at 45°C for 48 h with agitation as a chemical method. These steps in the chemical method were repeated as three cycles. The samples were washed in 1× PBS, and then incubated twice in a nuclease solution consisting of DNase I in 50 mM tris-HCl and 50 mg/mL BSA buffer for 4 h at 37°C in the enzymatic treatment step. Hypertonic buffer was used as a final incubation step, then samples were washed with 1× PBS for 24 h at room temperature. For the sterilization step, samples were incubated in 0.01% peracetic acid for 3 h. Finally, bone tissues were washed twice in PBS at 37°C and 25°C for 24 h.

Characterization of the decellularization process

Histological observations

Bone tissues were evaluated for histological characterization of the decellularized bone samples. Initially, tissue samples were fixed in 4% (*v*/*v*) neutral buffered formalin for 72 h and then dehydrated using the routine process before embedding in paraffin. 5 µm thick sections were prepared by using a microtome (Histocore Multicut, Leica Biosystems), and hematoxylin eosin (HE) staining was used to evaluate the general morphology of the cells and the ECM matrix of bone tissues. Besides, Masson Trichrome (MT) and Alizarin Red S (ARS) staining were used to observe collagen distribution and mineralization sites, respectively. Untreated native bones were used as controls in all stainings.

Fluorescence and SEM imaging

The cell nuclei of bone samples were assessed with 4',6-diamidino-2-phenylindole (DAPI, Invitrogen, USA) staining by fluorescence microscopy after the decellularization process. Tissues were fixed in 4% (*v*/*v*) formalin and then rinsed with 1× PBS. Cell nuclei were stained with DAPI for observation of the cell nuclei and observed by fluorescence microscopy (Carl Zeiss Observer D1). For the SEM imaging, untreated and decellularized bone samples were fixed with paraformaldehyde for 20 min at room temperature. Following washed with 1× PBS, samples were dehydrated in a graded ethanol series (50%, 70%, 80%, 90% and 100%), and then the samples were observed by SEM (Quanta 450 FEG SEM, Thermo Fisher Scientific).

Biochemical analyses

Total DNA content of untreated and decellularized bone tissues was determined after the decellularization process. Firstly, tissues were homogenized with DNeasy 96 Blood & Tissue Kit (Macherey-Nagel, GmbH&Co KG), following the manufacturer's protocol, and then DNA content of tissues was measured at 260/280 nm in a Nanodrop spectrophotometer (Nano 2000, Thermo Fisher Scientific).

The total collagen content of the tissues was quantified by hydroxyproline assay. Tissues were hydrolyzed by incubation with 6 M hydrochloric acid at 95°C for 20 h. The sample solutions and test standards were prepared according to the Quickzym (Biosciences) kit manual. The 96-well plate was prepared and incubated at 60°C for 60 min, then the absorbance at 570 nm was measured (Varioskan Flash, Thermo Fisher Scientific). The concentration of collagen was calculated by interpolation from the standard curve.

The GAG content was determined using the Sulfate Glycosaminoglycan Quantification Kit (Amsbio, AMS Biotechnology). After enzymatic digestion with papain at 60°C for 48 h, standard or test solutions were prepared according to the manufacturer's protocol. The absorbance at 530 nm was measured using a microplate reader (Varioskan Flash, Thermo Fisher Scientific). The resultant concentrations of sulfated sugars representative of GAG were determined by interpolation from the standard curve.

Biomechanical test

Biomechanical properties of the bones were evaluated with a compression test (Shimadzu Autograph AG-I, Shimadzu Co., Kyoto, Japan) according to ASTM-D 5024-95a standard. Native bones and decellularized bones (n = 6) were used, and tests were carried out with a 1 mm/min crosshead speed up to failure. The sample surface area was measured prior to the mechanical test. Young modulus was determined as the slope in the linear region from stress-strain curves, and maximum stress was calculated based on the strain and stress data.

In vitro cytocompatibility

Cell culture

Mouse preosteoblast MC3T3-E1 cells (Subclone 4 cells, ATCC) were used to examine the cytocompatibility of decellularized bone tissues. Mycoplasma test was routinely monitored using MycoAlert mycoplasma detection kit (Lonza), and all cultures used in experiments tested negative for mycoplasma. The cells were sub-cultured in alpha modified minimum essential medium (α-MEM) containing 10% fetal bovine serum (FBS), 1% penicillin/streptomycin, and L-glutamine at 37°C in a humidified 5% CO_2 atmosphere. Prior to cell seeding, the decellularized bone tissues were disinfected using 70% ethanol for an overnight addition to peracetic acid treatment in the decellularization step. Following the disinfection, samples were washed with 1× PBS thrice to remove residual ethanol, and then they were immersed in cell culture medium for 3 h at 37°C for conditioning. MC3T3-E1 cells (1×10^5 cells/scaffolds) were seeded on the decellularized bones ($1 \times 1 \times 0.3$ cm^3) and cultured for 28 days in α-MEM supplemented with 10% FBS, 1% penicillin/streptomycin, and L-glutamine at 37°C in a humidified atmosphere of 5% CO_2 in an incubator. The culture medium was refreshed twice a week during the incubation period. Cells seeded in a tissue culture plate (TCP) were used as a control group.

Cytotoxicity

For the in vitro cytotoxicity assessment, an indirect elution method by water-soluble tetrazolium salt (WST-1, Sigma Aldrich) colorimetric assay was used according to ISO-10993 standard. MC3T3-E1 cells (1×10^5 cells/scaffolds) were seeded on the decellularized bones ($1 \times 1 \times 0.3$ cm^3, n = 6) and incubated for 72 hours at 37°C in a humidified atmosphere of 5% CO_2 in an incubator. The absorbance was measured at 450 nm wavelength, and cell viability was calculated by using the following equation:

$$\text{Cell viability}\,(\%) = \frac{A_x}{A_0} \times 100$$

where A_x is the average absorbance value of treated samples; A_0 is the average absorbance value of control.

Cell proliferation

Cell proliferation on the decellularized bones was assessed with a WST-1 colorimetric assay by conversion of a water-soluble tetrazolium salt through cellular metabolism into an insoluble formazan. MC3T3-E1 cells (1×10^5 cells/scaffolds) were seeded onto disinfected decellularized bones (n = 6) and incubated for

28 days at 37°C in a humidified atmosphere of 5% CO_2. At each time point, cells on the decellularized bones were incubated with cell culture medium containing 1% (*v*/*v*) WST-1 solution for 4 hours. After incubation, the absorbance at 450 nm was recorded using a plate reader (Varioskan Flash, Thermo Fisher Scientific).

Cell morphology

MC3T3-E1 cells, incubated on dbECM substitutes for 14 days, were observed by fluorescence microscopy. After 14 days of incubation, cells were fixed with 4% (*v*/*v*) paraformaldehyde in PBS solution for 20 min at room temperature. Samples were washed with 1× PBS, and 0.1% Triton X-100 was used for permeabilization, then stained with DAPI and Alexa Fluor 555 (Invitrogen, Thermo Fisher Scientific) for observation of the cell nuclei and cytoskeleton, and visualized by fluorescence microscopy (Zeiss Scope A1).

In vitro osteogenic differentiation

Alkaline phosphatase activity

Alkaline phosphatase (ALP) activity of cells on the decellularized bone (n = 6) was quantified at 7, 14, 21, and 28 days. Cells on the decellularized bones were incubated with osteogenic medium (α-MEM containing 10% FBS, 1% penicillin/streptomycin, L-glutamine, 1 µL/mL L-ascorbic acid, 10 µL/mL β-glycerophosphate) for 28 days. Released ALP into the culture medium was measured spectrophotometrically by a plate reader at 405 nm according to the manufacturer's protocols (Biovision, Inc., USA).

Osteocalcin secretion

MC3T3-E1 cells were cultured on the decellularized rat and rabbit bone (n = 6) for 28 days of incubation time in osteogenic medium (α-MEM containing 10% FBS, 1% penicillin/streptomycin, L-glutamine, 1 µL/mL L-ascorbic acid, 10 µL/mL β-glycerophosphate). Osteocalcin secretion of cells was determined using the Osteocalcin ELISA Kit (Biovision). Culture media were collected and analyzed for the determination of the osteocalcin concentrations in accordance with the manufacturer's protocol.

Statistical analysis

All experiments were repeated thrice, and samples were evaluated in triplicate. The experimental data were represented as mean ± standard deviation (SD). The differences between groups in biochemical, biomechanical, and in vitro biocompatibility tests were analyzed using one-way analysis of variance (ANOVA) with Tukey's multiple comparison test. All p-values less than 0.05 were considered to be significant (* $p < 0.05$, ** $p < 0.01$, *** $p < 0.001$, **** $p < 0.0001$).

Results

Characterization of the decellularization process

After the decellularization process, bone tissues were stained with HE for general structural evaluation, MT for collagen distribution, and ARS for observation of mineralization sites. HE staining showed that round-shaped osteoblasts were observed in untreated native rat and rabbit bone tissue before decellularization, and cells localized in osteon structure were successfully removed from both rat and rabbit bone tissue after decellularization (Figure 2A, 2B). Figure 2 indicates that cell nuclei in untreated bone tissue before decellularization and cell lacunae were observed to be empty after decellularization. Also, magnified figures (on the right) display that circular osteon structures, which are important for cell localization and provide mechanical support to the bone tissue, were not affected by the decellularization process.

DNA content of both rabbit and rat bone tissues was evaluated spectrophotometrically. Total DNA content of rabbit bones was measured as 81.13 ± 12 ng/mL and 8.02 ± 0.4 ng/mL before and after decellularization, respectively (Figure 2C, Table S1). In rat bones, the total amount of DNA was measured as 29.92 ± 8 ng/mL and 4.93 ± 2 ng/mL before and after decellularization, respectively, and statistically significant differences were detected (*** $p < 0.001$) (Figure 2D, Table S1). After decellularization, 95.88% ± 0.16% for rabbit bone and 92.07% ± 0.45% for rat bone reduction in DNA content were achieved.

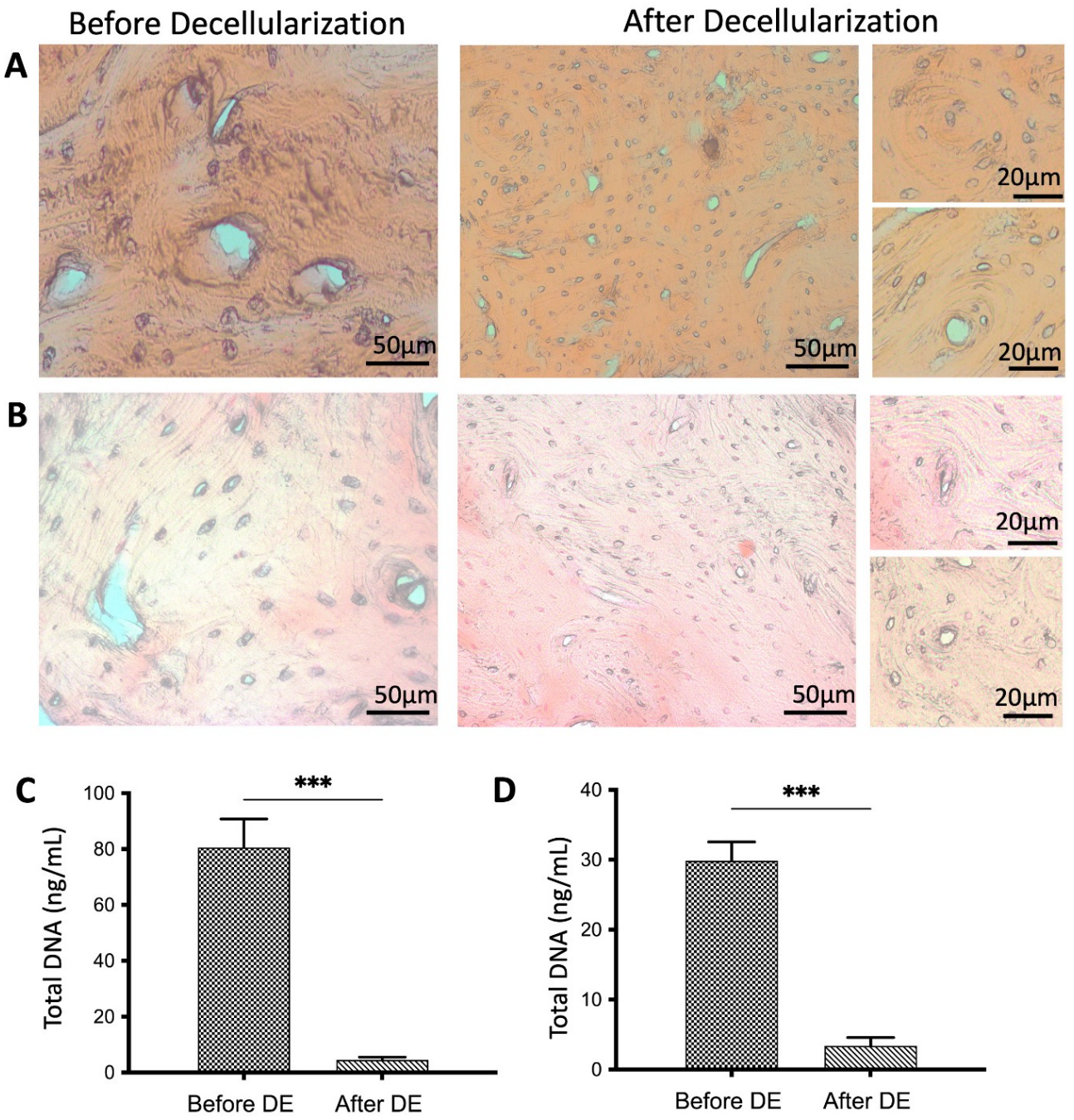

Figure 2. General morphology and DNA determination of the bone tissues. HE staining of rabbit (**A**) and rat (**B**) bone tissues before and after decellularization. DNA quantification results of rabbit (**C**) and rat (**D**) bone tissues (n = 6) before and after decellularization. Data are presented as mean ± SD (*** p < 0.001). DE: decellularization.

MT staining revealed that collagen structures were maintained in both decellularized rabbit and rat bone tissues and were observed in a radial direction around the empty lacuna after decellularization (Figure 3A, 3B). The total collagen content of the bone tissues was determined using a spectrophotometric method based on the amount of hydroxyproline. As shown in Figure 3C, the total collagen amount in rabbit bones decreased slightly from 55.53 ± 2.15 mg/mL to 48.72 ± 1.06 mg/mL after decellularization. In rat bones, it was measured as 37.8 ± 2.68 mg/mL before decellularization and 34.43 ± 4.45 mg/mL after decellularization (Figure 3D). As expected, there was no statistically significant difference observed in either bone sample. GAG amounts in the tissues were evaluated spectrophotometrically. As shown in Figure 3E and 3F, the GAG amounts in rabbit and rat bones were slightly reduced after decellularization, with no statistically significant difference found. According to the biochemical test results, it can be concluded that the DNA content in bone tissues was significantly reduced. However, the total amounts of collagen and GAG in the bone tissues were preserved.

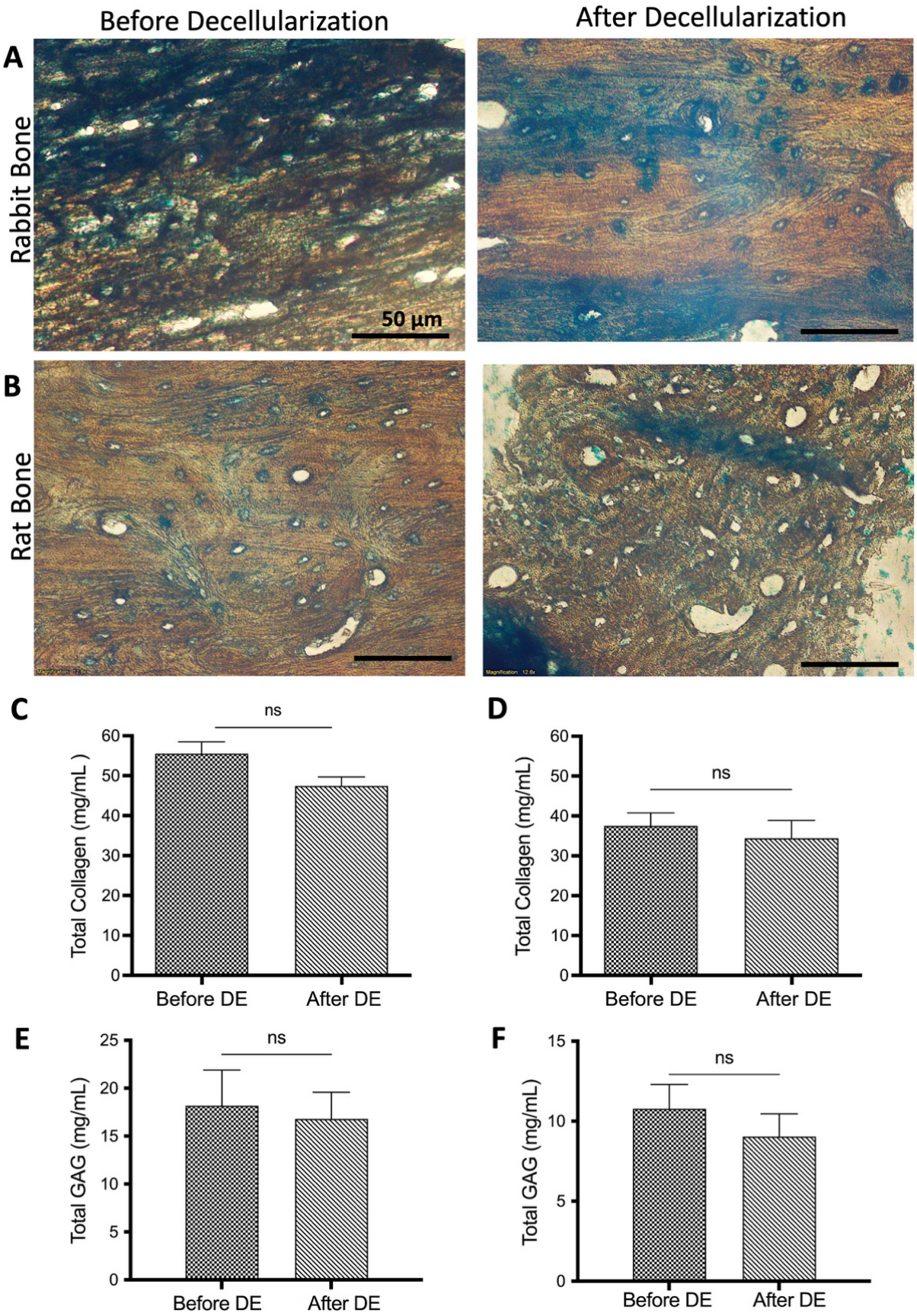

Figure 3. Total collagen and GAG determination of the bone tissues. MT staining of rabbit (**A**) and rat (**B**) bone tissues before and after decellularization. Scale bar: 50 μm. Total collagen quantification results of rabbit (**C**) and rat (**D**) bone tissues (*n* = 6). Total GAG amount of rabbit (**E**) and rat (**F**) bone tissues (*n* = 6) before and after decellularization. Data are presented as mean ± SD. DE: decellularization.

Mineralization sites of the bone tissues were observed as red/brown color in ARS staining (Figure 4A, 4B). In rabbit bone tissue, mineralization sites surrounding the osteon structures were clearly observed before and after decellularization, revealing no changes in the structures throughout the process (Figure 4A). In contrast, rat bone tissue displayed partially irregular structures after decellularization; however, the mineralization sites, indicated by a brown color, remained unchanged (Figure 4B). The tissue volume and density of rabbit and rat bones show differences as reported previously [42]. Also, due to the smaller size of rat bones, it might be possible to observe damage than in rabbit bone. This might be the reason that we found partial damage in the rat tissue. Moreover, the FTIR spectrum showed the inorganic and organic compounds of both rabbit and rat bones preserved after decellularization (Figure S1).

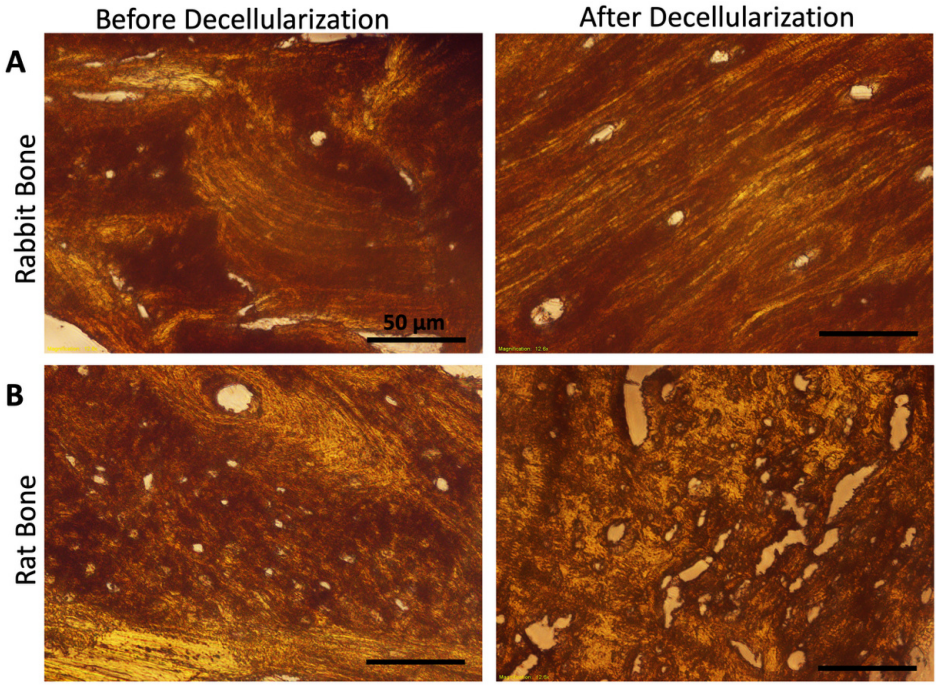

Figure 4. Evaluation of the mineralization site of the bone tissues. ARS staining of rabbit (**A**) and rat (**B**) bone tissues before and after decellularization. Scale bar: 50 µm.

Fluorescence and SEM imaging

DAPI staining was used to observe the cells in the bone tissues for fluorescence imaging. Cell distribution was observed homogenously on the untreated rabbit and rat bone tissues as control groups (Figure 5A). Especially, cells were localized around round-shaped osteon structures as seen in bright blue color. After the decellularization process, no cell nuclei in the decellularized bone tissues were found as expected. Similar to histological results, fluorescence imaging indicated the removal of the cellular components from the bone tissues successfully with the decellularization process.

SEM analysis revealed the surface morphology of rabbit and rat bones, both before and after decellularization. Figure 5B illustrates the overall bone structure, including the Haversian canal centrally located within the osteons and the canaliculi present in both rabbit and rat samples, suggesting that the micro-histoarchitecture of the bone tissue remained intact following decellularization.

Biomechanical analysis

Untreated and decellularized bone tissues were tested under compression to determine their compressive properties. The maximum compression force that could be applied to untreated bone tissue was determined as 162.02 ± 11.81 *N* for rabbit bone and 49.78 ± 8.72 *N* for rat bone before decellularization. These values slightly decreased to 153.83 ± 10.57 *N* and 42.72 ± 9.53 *N* after decellularization (Figure 6). No statistically significant differences were found before and after decellularization. The compression strength of untreated rabbit and rat bone was determined to be 17.95 ± 2.05 MPa and 11.69 ± 1.21 MPa,

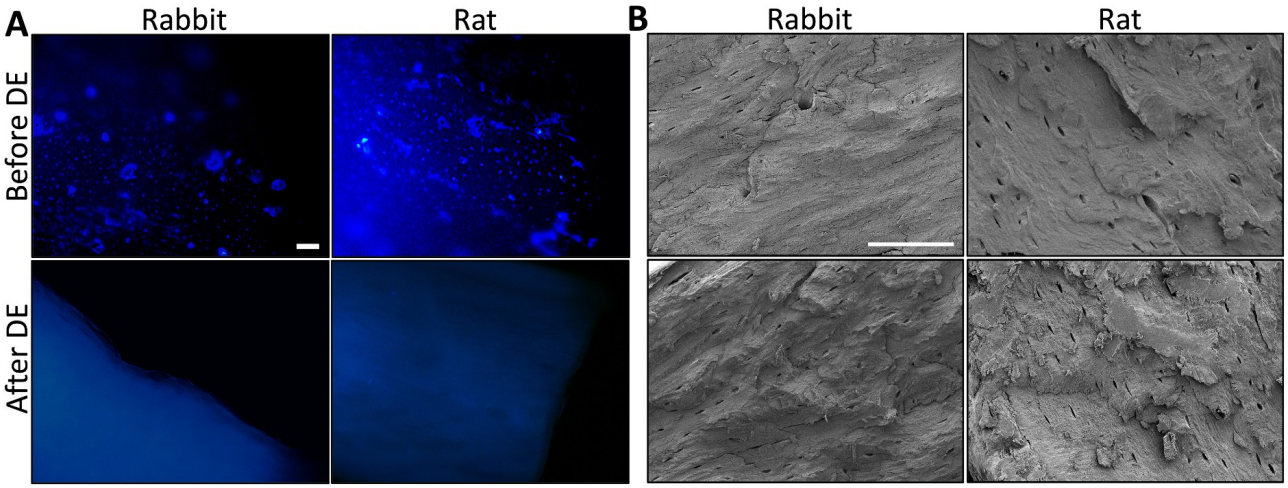

Figure 5. General morphology and nuclei evaluation of the bone tissues. Fluorescence (**A**) and SEM (**B**) imaging of the rabbit and rat bone tissue before and after decellularization. Scale bars: 100 μm (**A**), 100 μm (**B**). DE: decellularization.

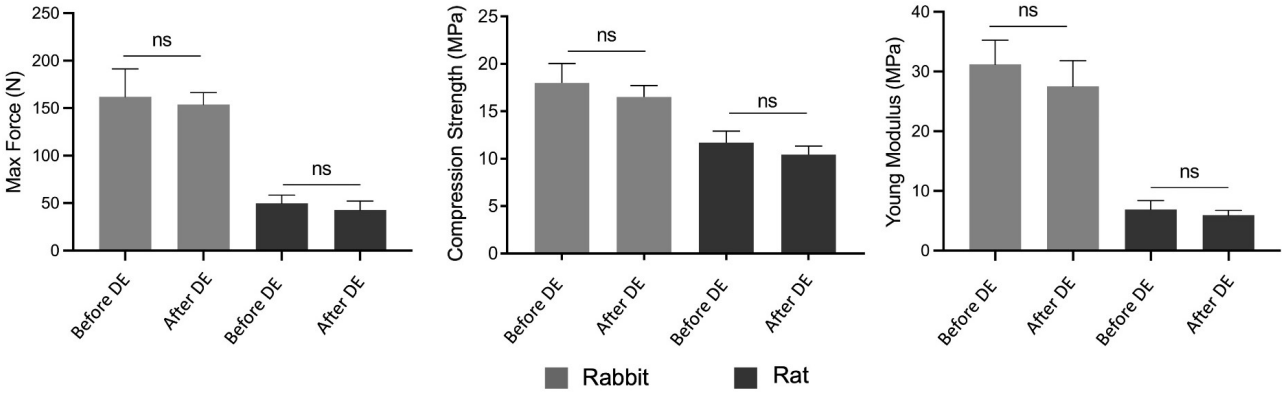

Figure 6. Biomechanical test results of rabbit and rat bone tissues before and after decellularization. The tests were performed using six replicates (n = 6) and data represented as mean ± SD. DE: decellularization.

respectively. After decellularization, the compression strength of the bone tissues did not change significantly, and there were no statistical differences before and after decellularization (Figure 6). Additionally, the Young's modulus of the bones was determined before and after decellularization. The Young's modulus of both bone tissues did not change much after decellularization. Furthermore, no statistically significant difference was found for Young's modulus, confirming that the decellularization did not affect the biomechanical properties of the bones (Figure 6).

Recellularization study of decellularized bone tissues

To evaluate the cytocompatibility of the dbECM, MC3T3-E1 cells were incubated for a 28-day culture period. Figure 7 depicts the fluorescence images of the cells covered on the decellularized substitutes on day 14 of the culture; the cell nuclei and cytoskeleton are shown in blue and green, respectively. The cells were spread and distributed homogeneously on the surface of the dbECM substitutes. The finding of the indirect cytotoxicity test showed that cells maintained their viability, and the decellularization process and dbECM substitutes had no influence on growing MC3T3-E1 cells. There were statistically significant differences found at 24, 48, and 72 h for both rat and rabbit dbECM; however, there was no statistically significant difference detected between rat and rabbit dbECM after 72 h incubation. The proliferation assay results showed that cells proliferated with an increasing trend for both rat and rabbit dbECM. It was determined that the proliferation capacity of the cells on dbECM substitutes was higher in comparison to the TCP control, also cell proliferation for rabbit dbECM was higher than rat dbECM. The significant differences were found on days 21 and 28 of culture between TCP and dbECM groups. Thus, it is estimated that the dbECM substrates would increase the cellular activity in a natural microenvironment as a natural substrate. The viability and proliferation results indicate that the dbECM substrates could be accepted as

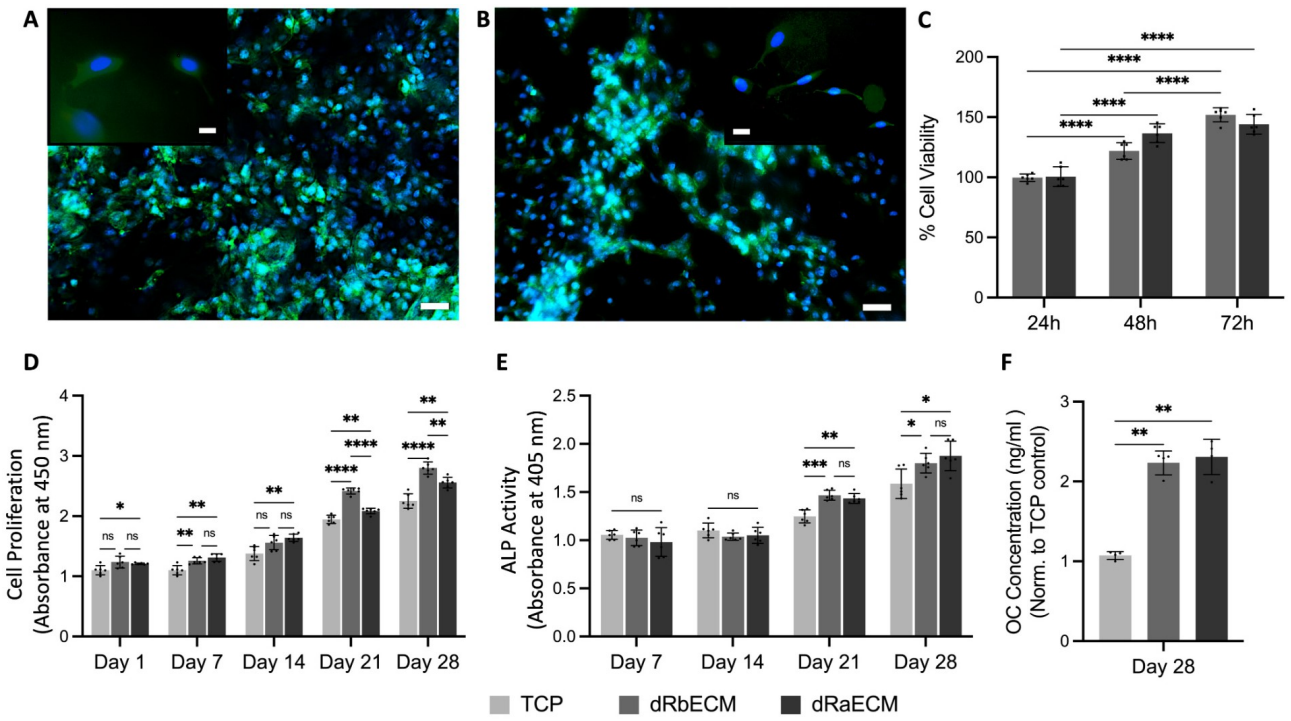

Figure 7. Recellularization study of decellularized rabbit dbECM (dRbECM) and rat dbECM (dRaECM). Fluorescence microscopy images of the cell-seeded dRbECM (**A**) and dRaECM (**B**) on 14 days of the culture period. Scale bars: 50 µm, 20 µm (inlets). Cytotoxicity of the decellularized bones according to cell viability (%) of the elution test (**C**). Proliferation (**D**), ALP activity (**E**), and osteocalcin (OC) secretion (**F**) of the cells on dbECM during 28 days of incubation. All assays were performed using six replicates (n = 6), and data are shown as mean ± SD (* $p < 0.05$, ** $p < 0.01$, *** $p < 0.001$, **** $p < 0.0001$).

biocompatible and have the potential for cell growth. Although MC3T3-E1 cells are of murine origin, they exhibited high proliferation capacity on both decellularized rabbit bone extracellular matrix (dRbECM) and decellularized rat bone extracellular matrix (dRaECM), indicating that the decellularization process was effective in minimizing immunological responses, which was one of the main aspects of the decellularization of the tissues. Also, cells showed better growth on dRbECM when compared to the dRaECM substrates. The implications of this result in selecting optimal substrates for bone tissue engineering, suggesting that rabbit dbECM may provide a more favorable microenvironment for osteoblast proliferation and thus could be considered a more suitable substrate. Furthermore, ALP activity was also assessed on dbECM substitutes. ALP release by the cells was stable on days 7 and 14 for each group; however, it was increased on day 21 of culture, and statistically significant differences were found between TCP and both dRbECM and dRaECM on the 21st-day incubation. Also, both rat and rabbit dbECM reached the maximum ALP release on the 28th day of culture, and there were statistical differences compared to the TCP control group. On the other hand, secretion of osteocalcin was determined, and since the MC3T3-E1 pre-osteoblast cells had differentiation capacity, the higher osteocalcin secretion was detected in both rat and rabbit recellularized bones on day 28 of the culture period (Figure 7F). Cell differentiation studies revealed that both dRaECM and dRbECM induce higher secretion of ALP and osteocalcin by MC3T3-E1 cells compared to TCP control (Figure 7E, 7F). The results of these two markers confirmed the osteogenic effectiveness of decellularized bone substitutes due to HAp content.

Discussion

The decellularized scaffold utilizes the natural three-dimensional architecture of tissues to create scaffolding materials suitable for tissue engineering and regenerative medicine. Physical decellularization methods, including repeated freeze-thaw cycles and high-pressure treatments, often fail to completely eliminate cellular debris, potentially triggering immunogenic reactions. To address these limitations, various techniques have been developed [43–45]. Among them, a combination of Triton X-100 and SDS has proven most effective in cellular component removal; however, its impact on the ECM components has been noted [26]. Additionally, SDS, Triton X-100, and TnBP are commonly used to remove cells and cellular

debris from bone and other tissues [46, 47]. SDS, in particular, demonstrates superior efficiency in cellular component removal compared to Triton X-100 and TnBP [48]. Despite its effectiveness, chemical decellularization, though yielding the best results among available methods, has been observed to alter the biomechanical properties of tissues due to ECM degradation [49, 50]. Such biomechanical changes can negatively impact cellular activity and the regenerative capacity of the tissue. The development of scaffolds using decellularized bone has been motivated by the need to enhance the biocompatibility of allograft bone while preserving its native structure.

Bone tissue has a unique composition, including osteon structures, Haversian and Volkmann's canals, and specialized cell types. The osteon, the fundamental unit of cortical bone, consists of concentric lamellae composed of osteoblasts and osteocytes surrounding a central Haversian canal containing blood vessels [51]. Due to this compact, layered structure, removing cellular components from bone proves more challenging than from other tissues. A combination of treatments can enhance decellularization efficiency while maintaining the natural ECM. In this study, a novel decellularization method incorporating physical, chemical, and enzymatic treatments successfully cleared cellular components from rat and rabbit bone tissue. Histological HE staining confirmed cellular component removal while preserving the circular osteon structures critical for cell localization (Figure 2). Furthermore, DNA assays validated the effective removal of DNA from both rabbit and rat bone tissue (Figure 2C, 2D). After decellularization, DNA content was measured at 8.02 ± 0.4 ng/mL and 4.93 ± 2 ng/mL, respectively. These values are significantly below the recommended upper limit of 50 ng DNA for complete decellularization [18]. Laker et al. [47] found that using combined detergents enhances decellularization effectiveness compared to SDS alone, as excessive SDS exposure can damage ECM integrity. However, in this study, an optimized SDS concentration of 0.1% enabled effective decellularization while minimizing ECM degradation. This approach achieved a 95% and 92% reduction in DNA content for rabbit and rat bone, respectively, aligning with DNA removal efficiencies reported by Yates et al. [52] and Ibrahim et al. [53]. Unlike previous methods relying solely on washing steps that degrade proteins and disrupt ECM structure, the present decellularization process integrates physical, chemical, and enzymatic treatments, achieving high DNA removal without significant ECM protein loss.

Preservation of ECM proteins is another critical factor in evaluating decellularization effectiveness. Collagen and GAG content remained largely intact following the decellularization process, as confirmed by histological and biochemical analyses. Collagen, the primary ECM structural component, provides tensile strength, supports cell adhesion, and facilitates cell proliferation [54, 55]. Studies indicate that SDS and Triton X-100 have milder effects on ECM integrity than trypsin, which leads to substantial ECM component loss [56, 57]. MT staining confirmed the retention of collagen structures after decellularization (Figure 3), while SEM further demonstrated the preservation of collagen fibers, indicating that bone tissue microarchitecture remained unaltered (Figure 5). Additionally, biochemical assays verified that total collagen and GAG content were preserved after decellularization (Figure 3C–3F). Literature reports highlight varying ECM molecule preservation across different decellularization methods, with SDS and Triton X-100 treatments often resulting in GAG reduction [28, 58, 59]. Xu et al. [60] demonstrated that among different detergents tested on annulus fibrosus tissue, trypsin caused the greatest GAG loss, followed by SDS and Triton X-100, with the latter achieving successful decellularization while maintaining macroscopic structure. The present method effectively preserved collagen and GAG content, representing a key achievement in maintaining bone ECM integrity.

Bone mineralization, a defining feature of bone tissue, has often been overlooked in decellularization studies [32, 34]. On the other hand, there are several studies that combine decellularization and demineralization processes in the literature [3, 38, 39, 61]. However, removing inorganic components, which are essential for osteoinductivity, can hinder cellular function in bone regeneration. This study evaluated bone mineralization sites post-decellularization to assess osteogenic activity and osteoinductivity. Histological staining confirmed that mineralization sites remained intact in both rat and rabbit bone samples (Figure 4), further supporting the bioactivity retention of the decellularized bone matrix.

Biomechanical properties are crucial for structural stability and scaffold functionality. Decellularized scaffolds provide a complex biochemical and mechanical environment that guides cell adhesion, proliferation, and differentiation. Bracey et al. [4] achieved 98% DNA content reduction in decellularized bone scaffolds using 0.05% trypsin and 2% Triton X-100; however, mechanical properties declined, resulting in reduced Young's modulus and stiffness [4]. In contrast, the present method maintained both maximum force and Young's modulus of rat and rabbit bones post-decellularization, with no statistically significant differences compared to untreated samples after 0.1% SDS treatment. These findings confirm that the decellularization process preserved bone histoarchitecture and mechanical strength (Figures 5 and 6).

Recellularization approach of the decellularized tissue is a critical step for the clinical usage of the decellularized ECM. Biocompatibility of the decellularized scaffolds, such as adipose tissue, skin, cartilage, meniscus, myocardium, pancreas, etc. has been investigated for the tissue regeneration capacity [30, 62–67]. As is known, the bioactive components induce the cellular activity, the preserved ECM components (i.e., collagen, proteoglycans) of the bone after the decellularization process have been shown to allow proliferation and differentiation of the osteoblasts [68]. In our recellularization study, fluorescence images confirmed that dbECM could support cell attachment as the cells attached, elongated, and spread on dRaECM and dRbECM surfaces (Figure 7A, 7B). Also, preosteoblasts proliferated on the dbECM and did not show any cytotoxicity (Figure 7C, 7D). Furthermore, ALP activity, known as an important osteogenic differentiation marker at early stages of bone regeneration, was also assessed on dbECM substitutes [69, 70]. The main structure of bone preserved after decellularization induced osteoblast differentiation by promoting cell attachment and proliferation as well as ALP secretion (Figure 7E). On the other hand, secretion of osteocalcin, which is the osteogenic marker for bone tissue, was determined [71, 72]. Since the MC3T3-E1 pre-osteoblast cells have differentiation capacity, the higher OC secretion was detected in both rat and rabbit recellularized bones on day 28 of the culture period (Figure 7F). Besides the cell differentiation capacity, it was estimated that HAp content of the decellularized bones also induced the osteocalcin secretion and osteogenic differentiation. The increasing ALP activity and the osteocalcin secretion of MC3T3-E1 pre-osteoblasts on dbECM substrates may be attributed to collagen fibers and HAp content, as well as residual growth factors preserved after the decellularization process. Previously reported studies showed that dbECM has the ability to retain biochemical signaling molecules such as growth factors, cytokines, and also induces cell differentiation [73, 74]. Cell differentiation studies revealed that both dRaECM and dRbECM induce higher secretion of ALP and osteocalcin by MC3T3-E1 cells compared to TCP control (Figure 7E, 7F). Although ALP is typically considered an early marker of osteogenic differentiation, we observed a high level of ALP activity on day 28, which aligns with elevated osteocalcin levels. This result may be attributed to the osteoinductive nature of the decellularized bone ECM, which can provide sustained biochemical cues that prolong or modulate the temporal pattern of osteogenic marker expression. Previous studies have reported similar trends in ECM-based scaffolds, where ALP activity remained high or peaked at later stages of differentiation [75–77]. These findings suggest that the bone-derived ECM not only supports early osteogenic commitment but may also enhance later stages of maturation and mineralization. The results of these two markers confirmed the osteogenic effectiveness of decellularized bone substitutes due to HAp content. Mattioli-Belmonte et al. [37] reported successful cellular removal from the tissue with decellularization and demineralization methods. It was determined a significant increase in collagen and osteonectin, as well as a significant decrease in ALP and osteocalcin after 14 days of cell culture [37]. Unlike our method, the decellularization process, including demineralization or decalcification of the tissues, might affect the recellularization process in accordance with changing the biomineralization feature of the tissue; thus, this could lead to a decrease in the secretion of osteogenic markers.

Considering all these results, the presented study demonstrated that cellular components were removed from the bone tissue, and ECM proteins and inorganic components were preserved without any significant change in the mechanical properties. Therefore, the method developed in the present study is favorable to the development of biological bone scaffolds, may be a promising candidate for use in bone

regeneration. Decellularized bone scaffolds possess biochemical and mechanical properties and have the potential for clinical use in the future.

Moreover, the biological activity of dbECM is a promising biomaterial for bone tissue engineering due to its native bioactivity, osteoinductivity, and structural support for cell attachment and differentiation. It can be used as a substrate for bone regeneration, a reinforcement in bioinks for 3D bioprinting, and as a physiologically relevant substrate for in vitro models. Future developments aim to standardize production, enhance mechanical and biological performance through hybrid materials, and enable personalized therapies. Ongoing research also focuses on optimizing immune compatibility and translating these materials into clinical applications.

Conclusions

Decellularization is a highly effective method for the development of natural biological ECM for tissue regeneration. Specifically, decellularized bone tissue serves as an ideal scaffold for bone tissue regeneration due to its excellent structural and mechanical properties and lack of immunogenicity. We developed a novel and efficient decellularization process to generate biological bone ECM for bone regeneration. Our method preserves both the organic and inorganic components of bone tissue. To the best of our knowledge, this is the first study to assess both the inorganic and organic content of decellularized bone, demonstrating the ability to obtain biocompatible bone scaffolds with minimal chemical exposure and short incubation times compared to existing methods. Our results confirm the successful removal of cellular components while maintaining key ECM elements, including collagen, GAG, and mineralization sites. Notably, the mechanical strength of the bone remained unchanged after decellularization. Biocompatibility assays further revealed that cells proliferated on the decellularized bone and differentiated into osteoblasts over a 28-day culture period, indicating that the scaffold supports osteogenic differentiation in vitro. Decellularized ECM scaffolds derived from rabbit and rat bones demonstrated strong potential for bone regeneration due to the inductive effects of ECM-derived molecules on cellular adhesion, proliferation, and differentiation. Additionally, our findings highlight the importance of preserving bone mineralization as a key factor in osteogenic activity. Overall, our method offers a promising approach for developing biological bone substitutes, which may serve as effective bone graft alternatives for clinical applications in the future.

Abbreviations

ARS: Alizarin Red S

DAPI: 4',6-diamidino-2-phenylindole

dbECM: decellularized bone extracellular matrix

dRaECM: decellularized rat bone extracellular matrix

dRbECM: decellularized rabbit bone extracellular matrix

ECM: extracellular matrix

FBS: fetal bovine serum

GAG: glycosaminoglycan

HAp: hydroxyapatite

HE: hematoxylin eosin

MT: Masson Trichrome

OC: osteocalcin

TCP: tissue culture plate

TnBP: *tri*-*n*-butyl phosphate

α-MEM: alpha modified minimum essential medium

Supplementary materials

The supplementary figure and table for this article are available at: https://www.explorationpub.com/uploads/Article/file/101345_sup_1.pdf.

Declarations

Acknowledgments

The authors are grateful to the Izmir Institute of Technology Biotechnology and Bioengineering Research and Application Center (IZTECH BIOMER) and Center for Materials Research (IZTECH MAM) for fluorescence analysis, microtome sectioning, histological imaging, and SEM imaging.

Author contributions

AKÖ: Conceptualization, Investigation, Writing—original draft, Writing—review & editing. HH: Conceptualization, Validation, Writing—review & editing. FT: Conceptualization, Validation, Writing—review & editing, Supervision. All authors read and approved the submitted version.

Conflicts of interest

The authors declare that they have no conflicts of interest.

Ethical approval

The study was approved by the Animal Experiments Ethical Committee of the Dokuz Eylul University School of Medicine, Izmir, Turkey (Protocol No: 44/2019). The study complies with the Guide for the Care and Use of Laboratory Animals.

Consent to participate

Not applicable.

Consent to publication

Not applicable.

Availability of data and materials

The raw data supporting the conclusions of this manuscript will be made available by the authors, without undue reservation, to any qualified researcher.

Funding

This research is supported by the Izmir Institute of Technology Scientific Research Project [2020-İYTE-0018]. Kara Özenler A. would like to thank Council of Higher Education (CoHE) (YÖK) for the scholarship YÖK 100/2000 PhD Biomaterials and Tissue Engineering. The funders had no role in study design, data collection and analysis, decision to publish, or preparation of the manuscript.

Publisher's note

References

1. Ansari M. Bone tissue regeneration: biology, strategies and interface studies. Prog Biomater. 2019;8:223–37. [DOI] [PubMed] [PMC]

2. Calori GM, Mazza E, Colombo M, Ripamonti C. The use of bone-graft substitutes in large bone defects: any specific needs? Injury. 2011;42:S56–63. [DOI] [PubMed]
3. Oryan A, Kamali A, Moshiri A, Eslaminejad MB. Role of Mesenchymal Stem Cells in Bone Regenerative Medicine: What Is the Evidence? Cells Tissues Organs. 2017;204:59–83. [DOI] [PubMed]
4. Bracey DN, Seyler TM, Jinnah AH, Lively MO, Willey JS, Smith TL, et al. A Decellularized Porcine Xenograft-Derived Bone Scaffold for Clinical Use as a Bone Graft Substitute: A Critical Evaluation of Processing and Structure. J Funct Biomater. 2018;9:45. [DOI] [PubMed] [PMC]
5. Bracey DN, Jinnah AH, Willey JS, Seyler TM, Hutchinson ID, Whitlock PW, et al. Investigating the Osteoinductive Potential of a Decellularized Xenograft Bone Substitute. Cells Tissues Organs. 2019; 207:97–113. [DOI] [PubMed] [PMC]
6. Rossi F, Santoro M, Perale G. Polymeric scaffolds as stem cell carriers in bone repair. J Tissue Eng Regen Med. 2015;9:1093–119. [DOI] [PubMed]
7. Qu H, Fu H, Han Z, Sun Y. Biomaterials for bone tissue engineering scaffolds: a review. RSC Adv. 2019; 9:26252–62. [DOI] [PubMed] [PMC]
8. Rajangam T, An SSA. Fibrinogen and fibrin based micro and nano scaffolds incorporated with drugs, proteins, cells and genes for therapeutic biomedical applications. Int J Nanomedicine. 2013;8: 3641–62. [DOI] [PubMed] [PMC]
9. Kruger TE, Miller AH, Wang J. Collagen scaffolds in bone sialoprotein-mediated bone regeneration. Sci World J. 2013;2013:812718. [DOI] [PubMed] [PMC]
10. Denry I, Kuhn LT. Design and characterization of calcium phosphate ceramic scaffolds for bone tissue engineering. Dent Mater. 2016;32:43–53. [DOI] [PubMed] [PMC]
11. Gloria A, Santis RD, Ambrosio L. Polymer-based composite scaffolds for tissue engineering. J Appl Biomater Biomech. 2010;8:57–67. [PubMed]
12. Nikolova MP, Chavali MS. Recent advances in biomaterials for 3D scaffolds: A review. Bioact Mater. 2019;4:271–92. [DOI] [PubMed] [PMC]
13. Lin X, Patil S, Gao Y, Qian A. The Bone Extracellular Matrix in Bone Formation and Regeneration. Front Pharmacol. 2020;11:757. [DOI] [PubMed] [PMC]
14. Badylak SF, Kropp B, McPherson T, Liang H, Snyder PW. Small intestinal submucosa: a rapidly resorbed bioscaffold for augmentation cystoplasty in a dog model. Tissue Eng. 1998;4:379–87. [DOI] [PubMed]
15. Badylak SF, Freytes DO, Gilbert TW. Extracellular matrix as a biological scaffold material: Structure and function. Acta Biomater. 2009;5:1–13. [DOI] [PubMed]
16. Badylak SF, Freytes DO, Gilbert TW. Reprint of: Extracellular matrix as a biological scaffold material: Structure and function. Acta Biomater. 2015;23:S17–26. [DOI] [PubMed]
17. Fernández-Pérez J, Ahearne M. The impact of decellularization methods on extracellular matrix derived hydrogels. Sci Rep. 2019;9:14933. [DOI] [PubMed] [PMC]
18. Crapo PM, Gilbert TW, Badylak SF. An overview of tissue and whole organ decellularization processes. Biomaterials. 2011;32:3233–43. [DOI] [PubMed] [PMC]
19. Chen F, Yoo JJ, Atala A. Acellular collagen matrix as a possible “off the shelf” biomaterial for urethral repair. Urology. 1999;54:407–10. [DOI] [PubMed]
20. Verstegen MMA, Willemse J, van den Hoek S, Kremers G, Luider TM, van Huizen NA, et al. Decellularization of Whole Human Liver Grafts Using Controlled Perfusion for Transplantable Organ Bioscaffolds. Stem Cells Dev. 2017;26:1304–15. [DOI] [PubMed]
21. Armour AD, Fish JS, Woodhouse KA, Semple JL. A comparison of human and porcine acellularized dermis: interactions with human fibroblasts in vitro. Plast Reconstr Surg. 2006;117:845–56. [DOI] [PubMed]
22. Luc G, Charles G, Gronnier C, Cabau M, Kalisky C, Meulle M, et al. Decellularized and matured esophageal scaffold for circumferential esophagus replacement: Proof of concept in a pig model. Biomaterials. 2018;175:1–18. [DOI] [PubMed]

23. Gilbert TW, Sellaro TL, Badylak SF. Decellularization of tissues and organs. Biomaterials. 2006;27: 3675–83. [DOI] [PubMed]
24. Faulk DM, Badylak SF. Natural biomaterials for regenerative medicine applications. In: Orlando G, Lerut J, Soker S, Stratta RJ, editors. Regenerative medicine applications in organ transplantation. Boston: Academic Press; 2014. pp. 101–12. [DOI]
25. Chen G, Lv Y. Decellularized Bone Matrix Scaffold for Bone Regeneration. Methods Mol Biol. 2018; 1577:239–54. [DOI] [PubMed]
26. Woods T, Gratzer PF. Effectiveness of three extraction techniques in the development of a decellularized bone-anterior cruciate ligament-bone graft. Biomaterials. 2005;26:7339–49. [DOI] [PubMed]
27. Cartmell JS, Dunn MG. Effect of chemical treatments on tendon cellularity and mechanical properties. J Biomed Mater Res. 2000;49:134–40. [DOI] [PubMed]
28. Kim YS, Majid M, Melchiorri AJ, Mikos AG. Applications of decellularized extracellular matrix in bone and cartilage tissue engineering. Bioeng Transl Med. 2018;4:83–95. [DOI] [PubMed] [PMC]
29. Cartmell JS, Dunn MG. Development of cell-seeded patellar tendon allografts for anterior cruciate ligament reconstruction. Tissue Eng. 2004;10:1065–75. [DOI] [PubMed]
30. Kara A. Development of Meniscus Tissue Bio-Compatibility Using Allograft Native Scaffold [dissertation]. Izmir (Turk): Dokuz Eylül University; 2017.
31. Porzionato A, Stocco E, Barbon S, Grandi F, Macchi V, De Caro R. Tissue-Engineered Grafts from Human Decellularized Extracellular Matrices: A Systematic Review and Future Perspectives. Int J Mol Sci. 2018;19:4117. [DOI] [PubMed] [PMC]
32. Sawkins MJ, Bowen W, Dhadda P, Markides H, Sidney LE, Taylor AJ, et al. Hydrogels derived from demineralized and decellularized bone extracellular matrix. Acta Biomater. 2013;9:7865–73. [DOI] [PubMed] [PMC]
33. Lee DJ, Diachina S, Lee YT, Zhao L, Zou R, Tang N, et al. Decellularized bone matrix grafts for calvaria regeneration. J Tissue Eng. 2016;7:2041731416680306. [DOI] [PubMed] [PMC]
34. Rindone AN, Nyberg E, Grayson WL. 3D-Printing Composite Polycaprolactone-Decellularized Bone Matrix Scaffolds for Bone Tissue Engineering Applications. Methods Mol Biol. 2018;1577:209–26. [DOI] [PubMed]
35. Paduano F, Marrelli M, Alom N, Amer M, White LJ, Shakesheff KM, et al. Decellularized bone extracellular matrix and human dental pulp stem cells as a construct for bone regeneration. J Biomater Sci Polym Ed. 2017;28:730–48. [DOI] [PubMed]
36. Abedin E, Lari R, Shahri NM, Fereidoni M. Development of a demineralized and decellularized human epiphyseal bone scaffold for tissue engineering: A histological study. Tissue Cell. 2018;55:46–52. [DOI] [PubMed]
37. Mattioli-Belmonte M, Montemurro F, Licini C, Iezzi I, Dicarlo M, Cerqueni G, et al. Cell-Free Demineralized Bone Matrix for Mesenchymal Stem Cells Survival and Colonization. Materials (Basel). 2019;12:1360. [DOI] [PubMed] [PMC]
38. Fielding G, Bose S. SiO_2 and ZnO dopants in three-dimensionally printed tricalcium phosphate bone tissue engineering scaffolds enhance osteogenesis and angiogenesis in vivo. Acta Biomater. 2013;9: 9137–48. [DOI] [PubMed] [PMC]
39. Hsu EL, Ghodasra JH, Ashtekar A, Nickoli MS, Lee SS, Stupp SI, et al. A comparative evaluation of factors influencing osteoinductivity among scaffolds designed for bone regeneration. Tissue Eng Part A. 2013;19:1764–72. [DOI] [PubMed] [PMC]
40. Kara Özenler A. Development and characterization of novel bioink by using decellularized extracellular matrix for bone tissue engineering applications [dissertation]. Izmir (Turk): Izmir Institute of Technology; 2023.

41. American Veterinary Medical Association. AVMA Guidelines for the Euthanasia of Animals: 2020 Edition [Internet]. Schaumburg (IL): AVMA; c2020 [cited 2025 Jul 18]. Available from: https://www.avma.org/sites/default/files/2020-02/Guidelines-on-Euthanasia-2020.pdf
42. Bagi CM, Berryman E, Moalli MR. Comparative bone anatomy of commonly used laboratory animals: implications for drug discovery. Comp Med. 2011;61:76–85. [PubMed] [PMC]
43. Dong C, Lv Y. Application of Collagen Scaffold in Tissue Engineering: Recent Advances and New Perspectives. Polymers (Basel). 2016;8:42. [DOI] [PubMed] [PMC]
44. Gupta SK, Mishra NC, Dhasmana A. Decellularization Methods for Scaffold Fabrication. Methods Mol Biol. 2018;1577:1–10. [DOI] [PubMed]
45. Zhang W, Zhu Y, Li J, Guo Q, Peng J, Liu S, et al. Cell-Derived Extracellular Matrix: Basic Characteristics and Current Applications in Orthopedic Tissue Engineering. Tissue Eng Part B Rev. 2016;22:193–207. [DOI] [PubMed]
46. Kuna VK, Xu B, Sumitran-Holgersson S. Decellularization and Recellularization Methodology for Human Saphenous Veins. J Vis Exp. 2018;137:57803. [DOI] [PubMed] [PMC]
47. Laker L, Dohmen PM, Smit FE. Synergy in a detergent combination results in superior decellularized bovine pericardial extracellular matrix scaffolds. J Biomed Mater Res B Appl Biomater. 2020;108:2571–8. [DOI] [PubMed]
48. Xing S, Liu C, Xu B, Chen J, Yin D, Zhang C. Effects of various decellularization methods on histological and biomechanical properties of rabbit tendons. Exp Ther Med. 2014;8:628–34. [DOI] [PubMed] [PMC]
49. Lovati AB, Bottagisio M, Moretti M. Decellularized and Engineered Tendons as Biological Substitutes: A Critical Review. Stem Cells Int. 2016;2016:7276150. [DOI] [PubMed] [PMC]
50. Hoshiba T, Yamaoka T. Extracellular matrix scaffolds for tissue engineering and biological research. In: Yamaoka T, Hoshiba T, editors. Decellularized extracellular matrix: characterization, fabrication and applications. Cambridge: The Royal Society of Chemistry; 2019. pp. 1–14. [DOI]
51. Li M, Fu X, Gao H, Ji Y, Li J, Wang Y. Regulation of an osteon-like concentric microgrooved surface on osteogenesis and osteoclastogenesis. Biomaterials. 2019;216:119269. [DOI] [PubMed]
52. Yates P, Thomson J, Galea G. Processing of whole femoral head allografts: validation methodology for the reliable removal of nucleated cells, lipid and soluble proteins using a multi-step washing procedure. Cell Tissue Bank. 2005;6:277–85. [DOI] [PubMed]
53. Ibrahim T, Qureshi A, McQuillan TA, Thomson J, Galea G, Power RA. Intra-operative washing of morcellised bone allograft with pulse lavage: how effective is it in reducing blood and marrow content? Cell Tissue Bank. 2012;13:157–65. [DOI] [PubMed]
54. McIntosh L, van der Walle C. Control of Mammalian Cell Behaviour Through Mimicry of the Extracellular Matrix Environment. In: On Biomimetics. InTech; 2011. [DOI]
55. Rozario T, DeSimone DW. The extracellular matrix in development and morphogenesis: a dynamic view. Dev Biol. 2010;341:126–40. [DOI] [PubMed] [PMC]
56. Smith CA, Richardson SM, Eagle MJ, Rooney P, Board T, Hoyland JA. The use of a novel bone allograft wash process to generate a biocompatible, mechanically stable and osteoinductive biological scaffold for use in bone tissue engineering. J Tissue Eng Regen Med. 2015;9:595–604. [DOI] [PubMed]
57. Safdari M, Bibak B, Soltani H, Hashemi J. Recent advancements in decellularized matrix technology for bone tissue engineering. Differentiation. 2021;121:25–34. [DOI] [PubMed]
58. Mendoza-Novelo B, Avila EE, Cauich-Rodríguez JV, Jorge-Herrero E, Rojo FJ, Guinea GV, et al. Decellularization of pericardial tissue and its impact on tensile viscoelasticity and glycosaminoglycan content. Acta Biomater. 2011;7:1241–8. [DOI] [PubMed]
59. Petersen TH, Calle EA, Colehour MB, Niklason LE. Matrix composition and mechanics of decellularized lung scaffolds. Cells Tissues Organs. 2012;195:222–31. [DOI] [PubMed] [PMC]
60. Xu H, Xu B, Yang Q, Li X, Ma X, Xia Q, et al. Comparison of decellularization protocols for preparing a decellularized porcine annulus fibrosus scaffold. PLoS One. 2014;9:e86723. [DOI] [PubMed] [PMC]

61. Albrektsson T, Johansson C. Osteoinduction, osteoconduction and osseointegration. Eur Spine J. 2001; 10:S96–101. [DOI] [PubMed] [PMC]
62. Ibsirlioglu T, Elçin AE, Elçin YM. Decellularized biological scaffold and stem cells from autologous human adipose tissue for cartilage tissue engineering. Methods. 2020;171:97–107. [DOI] [PubMed]
63. Wolf MT, Daly KA, Brennan-Pierce EP, Johnson SA, Carruthers CA, D'Amore A, et al. A hydrogel derived from decellularized dermal extracellular matrix. Biomaterials. 2012;33:7028–38. [DOI] [PubMed] [PMC]
64. Bordbar S, Lotfi Bakhshaiesh N, Khanmohammadi M, Sayahpour FA, Alini M, Baghaban Eslaminejad M. Production and evaluation of decellularized extracellular matrix hydrogel for cartilage regeneration derived from knee cartilage. J Biomed Mater Res A. 2020;108:938–46. [DOI] [PubMed]
65. Kara A, Koçtürk S, Bilici G, Havitcioglu H. Development of biological meniscus scaffold: Decellularization method and recellularization with meniscal cell population derived from mesenchymal stem cells. J Biomater Appl. 2021;35:1192–207. [DOI] [PubMed]
66. Seo Y, Jung Y, Kim SH. Decellularized heart ECM hydrogel using supercritical carbon dioxide for improved angiogenesis. Acta Biomater. 2018;67:270–81. [DOI] [PubMed]
67. Sackett SD, Tremmel DM, Ma F, Feeney AK, Maguire RM, Brown ME, et al. Extracellular matrix scaffold and hydrogel derived from decellularized and delipidized human pancreas. Sci Rep. 2018;8:10452. [DOI] [PubMed] [PMC]
68. Blair HC, Larrouture QC, Li Y, Lin H, Beer-Stoltz D, Liu L, et al. Osteoblast Differentiation and Bone Matrix Formation In Vivo and In Vitro. Tissue Eng Part B Rev. 2017;23:268–80. [DOI] [PubMed] [PMC]
69. Murray E, Provvedini D, Curran D, Catherwood B, Sussman H, Manolagas S. Characterization of a human osteoblastic osteosarcoma cell line (SAOS-2) with high bone alkaline phosphatase activity. J Bone Miner Res. 1987;2:231–8. [DOI] [PubMed]
70. Fu C, Yang X, Tan S, Song L. Enhancing Cell Proliferation and Osteogenic Differentiation of MC3T3-E1 Pre-osteoblasts by BMP-2 Delivery in Graphene Oxide-Incorporated PLGA/HA Biodegradable Microcarriers. Sci Rep. 2017;7:12549. [DOI] [PubMed] [PMC]
71. Nakamura A, Dohi Y, Akahane M, Ohgushi H, Nakajima H, Funaoka H, et al. Osteocalcin secretion as an early marker of in vitro osteogenic differentiation of rat mesenchymal stem cells. Tissue Eng Part C Methods. 2009;15:169–80. [DOI] [PubMed]
72. Saldaña L, Bensiamar F, Boré A, Vilaboa N. In search of representative models of human bone-forming cells for cytocompatibility studies. Acta Biomater. 2011;7:4210–21. [DOI] [PubMed]
73. Prewitz MC, Seib FP, von Bonin M, Friedrichs J, Stißel A, Niehage C, et al. Tightly anchored tissue-mimetic matrices as instructive stem cell microenvironments. Nat Methods. 2013;10:788–94. [DOI] [PubMed]
74. Golebiowska AA, Intravaia JT, Sathe VM, Kumbar SG, Nukavarapu SP. Decellularized extracellular matrix biomaterials for regenerative therapies: Advances, challenges and clinical prospects. Bioact Mater. 2023;32:98–123. [DOI] [PubMed] [PMC]
75. Leferink AM, Santos D, Karperien M, Truckenmüller RK, van Blitterswijk CA, Moroni L. Differentiation capacity and maintenance of differentiated phenotypes of human mesenchymal stromal cells cultured on two distinct types of 3D polymeric scaffolds. Integr Biol (Camb). 2015;7:1574–86. [DOI] [PubMed]
76. Kara Özenler A, Distler T, Tihminlioglu F, Boccaccini AR. Fish scale containing alginate dialdehyde-gelatin bioink for bone tissue engineering. Biofabrication. 2023;15:025012. [DOI] [PubMed]
77. Yamada S, Yassin MA, Weigel T, Schmitz T, Hansmann J, Mustafa K. Surface activation with oxygen plasma promotes osteogenesis with enhanced extracellular matrix formation in three-dimensional microporous scaffolds. J Biomed Mater Res A. 2021;109:1560–74. [DOI] [PubMed]